ELSEVIER

Biochimica et Biophysica Acta 1317 (1996) 161–167

BBA Biochimica et Biophysica Acta

Structural and functional characterization of three human immunoglobulin κ light chains with different pathological implications

Vittorio Bellotti [a,*], Monica Stoppini [a], Palma P. Mangione [a], Alessandro Fornasieri [b], Li Min [b], Giampaolo Merlini [c], Giuseppina Ferri [a]

[a] *Department of Biochemistry University of Pavia, via Taramelli, 3b-27100 Pavia, Italy*
[b] *Department of Nephrology, Ospedale S. Carlo, Milan, Italy*
[c] *Biotechnology Research Laboratory IRCCS Policlinico S. Matteo, Pavia, Italy*

Received 29 May 1996; revised 15 August 1996; accepted 19 August 1996

Abstract

The structural properties of three immunoglobulins light chains: κ SCI, responsible for light chain deposition disease (Bellotti, V., Stoppini, M., Merlini, G., Zapponi, M.C., Meloni, M.L., Banfi, G. and Ferri, G. (1991) Biochim. Biophys. Acta 1097, 177–182), k INC responsible for light chain amyloidosis (Ferri, G., Stoppini, M., Iadarola, P., Bellotti, V. and Merlini, G. (1989) Biochim. Biophys. Acta 995, 103–108) and the non-pathogenic κ MOS were analyzed by fluorescence spectroscopy and circular dichroism.

Comparative evaluation of the data shows that SCI and MOS have similar stability under different conditions, while the amyloid k INC behaves as a very unstable protein.

As calculated from the GdnHCl curves, the midpoint of unfolding transition was 1.35 M for SCI, 1.20 M for MOS and 0.1 M for INC. Analysis of CD spectra evidences that the three proteins conserve their conformation in the range of pH 4–8. Change in temperature at pH 4.0 produces the premature transition of INC (T_m 40°C) with respect to SCI and MOS (T_m 50°C). At this pH both the pathological SCI and INC light chains aggregate at a temperature of 20°C lower than the normal counterpart. The specific kidney deposition of κ SCI has been evidenced after injection of the ^{125}I labelled light chain into mice. No deposition was detectable in the case of INC and MOS.

Keywords: Light chain; Light chain deposition disease; Amyloidosis; Unfolding

1. Introduction

Tissue deposition of immunoglobulin monoclonal light chain is characteristic of two distinct clinical entities: light chain (AL) amyloidosis and light chain deposition disease (LCDD). In the former disease the pathological light chain creates a typical fibrillar and Congo red birefringent aggregate in target tissues; in the latter the protein is localized in the basement membrane, without the fibrillar pattern [1]. The primary structure of pathogenic light chains has been extensively investigated in order to understand the molecular basis of this disease, and the aminoacid sequence of more than 60 amyloidogenic light chains has been reported so far. In contrast, only 4 light chains associated with LCDD have been completely sequenced [2–5].

The search for common structural functional characteristics of amyloidogenic light chains over the last few years has been unsatisfactory due to the extreme variability of the VL domain, although recurrent amino acid replacements have been identified in certain positions [6]. It has been reported that some of these mutations introduced into synthetic DNA encoding the VL domain of the non pathological REI light chain reduce protein stability and facilitate aggregation into amyloid-like fibrils [7]. Reduced stability seems to be a property not only of these mutants, but also of amyloidogenic transthyretin [8] and cystatin C [9]. The paucity of structural data regarding the immunoglobulins responsible for LCDD has not permitted the identification of putative pathogenic mutations and the

Abbreviations: LCDD, light chain deposition disease; GdnHCl, guanidine hydrochloride; p*I*, isoelectric point; PMSF, phenyl methyl sulfonylfluoride; PAS, periodic acid Schiff's reagent; DTT, dithiothreitol; CD, circular dichroism; T_m, midpoint of temperature unfolding transition; C_m, midpoint of GdnHCl unfolding transition; ECL, enhanced chemiluminescence

* Corresponding author. Fax: +39 0382 423108; e-mail: dbioc@unipv.it.

PII S0925-4439(96)00049-X

thermodynamic properties of these light chains are at the present unknown.

In this paper we present a comparative study on thermodynamic characterization and tissue distribution pattern in an in vivo model of a complete light chain (κ SCI) associated with LCDD and of an amyloidogenic light chain (κ INC), whose amino acid sequence were previously reported [2,10]. By way of comparison, we also studied the properties of a κ light chain clinically considered non pathological.

2. Materials and methods

2.1. Materials

Two immunoglobulin light chains responsible for LCDD (kSCI) [2] and AL amyloidosis (κ INC) [10] were purified from the urine of two patients submitted to periodical clinical check–ups. Diagnosis of the associated disease suggested by clinical presentation, was confirmed by specific tissue biopsy staining. The light chains κ MOS and λ GAR were referred as non pathological; neither the former, excreted at the level of 5 g/day, nor the latter excreted at the level of 17 g/day caused any syndrome associated with tissue deposition in three years of follow-up.

The following materials were obtained from commercial sources given in parentheses: reagents and protein standards for isoelectrophocusing and PAGE electrophoresis (Bio Rad Richmond, CA, USA); Superose G12 column, Sephadex G25 (Pharmacia, Uppsala, Sweden); ECL, $Na^{125}I$, $Na^{131}I$ (Amersham, Buckinghamshire, UK); Immobilon, acrodisc filters (Millipore, Bedford, MA, USA). Reagents used for automated sequence analysis were supplied by Hewlett-Packard (Palo Alto, CA, USA). All the other reagents were from Sigma (St. Louis, MO, USA).

2.2. Methods

2.2.1. Protein purification and structural analysis

Protein purification was conduced as previously reported by a combination of ammonium sulfate precipitation, ion exchange chromatography and gel filtration [2].

Size exclusion chromatography was performed at room temperature in a Superose G12 column using an FPLC apparatus; the column was equilibrated in 20 mM Tris-HCl, 0.15 M NaCl, pH 7.4.

SDS-PAGE in reducing and non-reducing conditions was carried out according to Laemmli [11] and stained with Coomassie blue and PAS.

Immunoblotting and isoelectrophocusing in 6 M urea were performed as previously described [12]. Standard proteins were used as p*I* markers.

The protein concentration was determined by amino acid analysis or spectrophotometrically at 280 nm with A1%/1 cm = 13.0.

Amino acid analysis was performed on a Kontron Chromakon 500 automated analyzer according to Moore [13].

The N-terminal sequence of κ MOS was determined by adsorptive biphasic column technology using an HPG1000A protein sequenator (Hewlett-Packard, Palo Alto, CA) with the routine 3.0 chemistry method and PTH_4M HPLC method.

2.2.2. Fluorescence measurements

Fluorescence spectra in the range 300–450 nm were measured with a Perkin Elmer LS50 spectrofluorimeter at 20°C on protein samples, 0.44 μM in 20 mM K phosphate buffer, pH 7.4. Thermodynamic stability of the light chains was determined by monitoring the dependence of intrinsic tryptophan fluorescence on GdnHCl concentration. The protein in the same solution was excited at 295 nm and emission was monitored at 345 nm [14]. The transition curves were analyzed as suggested by Finn et al. [15].

2.2.3. Circular dichroism

CD measurements were performed with a Jasco 710 spectropolarimeter equipped with a thermostated cell holder and a temperature controlled system. Temperature was monitored using a Microtherm 1006 thermometer and a S/N 117C temperature probe just outside the sample cell. Measurements were performed in cells with 0.1 cm and 1 cm path lengths in the far (190–250 nm) and in the near UV (250–310 nm), respectively.

Protein was dissolved in 20 mM K phosphate buffer at different pH and at a concentration of 2.2 μM (far UV) and 8.8 μM (near UV). The elipticity was recorded every 1 s with a response time of 1 s and a band width of 2 nm. Elipticities in deg cm^2 $dmol^{-1}$ were expressed as $[\theta]$. Thermal denaturation in the far UV region was monitored by calculating $[\theta]220 + [\theta]200$ and in the near UV region by measuring changes of $[\theta]$ at 280 nm. Elipticity readings were normalized to fraction unfolded (Fu) using the equation

$$Fu = [\theta] - [\theta]_N / [\theta]_U - [\theta]_N$$

where $[\theta]_U$ and $[\theta]_N$ represent respectively the elipticity values for the fully unfolded and fully folded state at each temperature.

2.2.4. Light scattering

Light scattering measurements were performed in a Perkin Elmer LS50 spectrofluorimeter equipped with a thermostated cell holder and a temperature controlled system. The aggregation was monitored in a temperature gradient. Samples were excited at 510 nm and the scattered light was detected at 90° to the incident beam; the spectral band was 2.5 nm. Protein concentration was 13.2 μM in 20 mM K phosphate buffer, pH 4.0. Signals were corrected for the blank value.

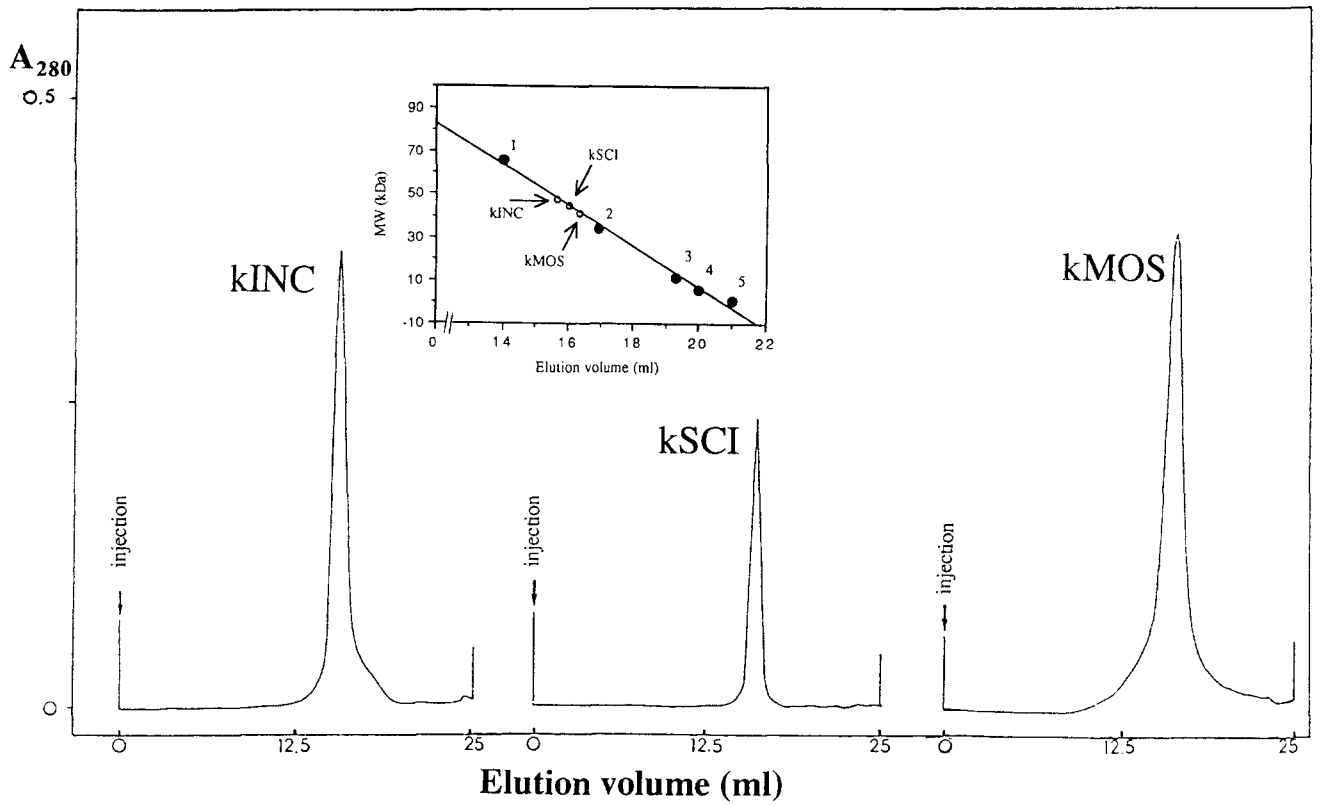

Fig. 1. Size exclusion chromatography of the light chains. Protein samples were subjected to size exclusion FPLC on a Superose G12 column. Elution was performed at room temperature, at a flow rate of 0.3 ml/min using 20 mM Tris-HCl, 0.15 M NaCl buffer, pH 7.4, as eluent. Inset: Molecular mass determination. Standard samples: 1 = bovine serum albumin (66 kDa), 2 = A1 protein (34 kDa), 3 = β-2-microglobulin (11.7 kDa), 4 = insulin (5.7 kDa) 5 = riboflavin (376 Da).

2.2.5. Fibrillogenesis and electron microscopy

Fibrillogenesis in vitro was carried out by submitting the insoluble precipitates of the light chains to pepsin digestion as suggested by Linke et al. [16]. Protein aggregate was directly visualized by electron microscopy on grids covered with a carbon-stabilized Formvar film after negative staining with 2% sodium phosphotungstate in water.

2.2.6. Quantitation of light chains deposition

Light chain deposition in mouse organs was evaluated following the method of Wilson and Dixon [17] with minor modifications. 2 mg of κ and 2 mg of λGAR light chain were labeled with ^{125}I and ^{131}I, respectively, using the chloramine-T method, and the free iodine was cleared by gel filtration on Sephadex G25. Free iodine was no more than 10% in the labelled protein preparation. 0.5 ml of a solution containing 0.5 mg of ^{125}I-κ light chain and 0.6 mg of ^{131}I-λ light chain in phosphate buffered saline (PBS), was injected via the tail vein in male BALB/c mice. After 1 h the mice were killed by exsanguination. Heparinized blood was collected, kidney, liver and spleen samples were weighted, diced and homogenized in a chilled Polytron homogenizer. The excess of radioactivity was eliminated by washing the precipitate with PBS. Radioactivity was determined in a gamma scintillation counter and the specific organ uptake of the radiolabelled probes was calculated by using the standard formula:

$$\text{specific organ}^{125}\text{I} = \frac{\text{organ}^{125}\text{I} - \text{organ}^{131}\text{I} \times \text{blood}^{125}\text{I}}{\text{blood}^{131}\text{I}}$$

2.2.7. Electrophoretic analysis of light chains extracted from the mouse kidney

In a separate experiment, 3 mice were injected with 0.5 ml of a solution of κ SCI, κ INC and κ MOS (1 mg/ml

Table 1
N-terminal sequence of κ MOS

1	D	I	Q	M	T	Q	S	P	S	T	L	S	A	S	V	G	D	R	V
20	I	I	T	C	R	A	S	Q	D	I	S	S	R	L	A	W	F	Q	Q
39	K	P	G	K	A	P	E	V	L	I	Y	D	A	S	I	L	Q	S	G
58	V	P																	

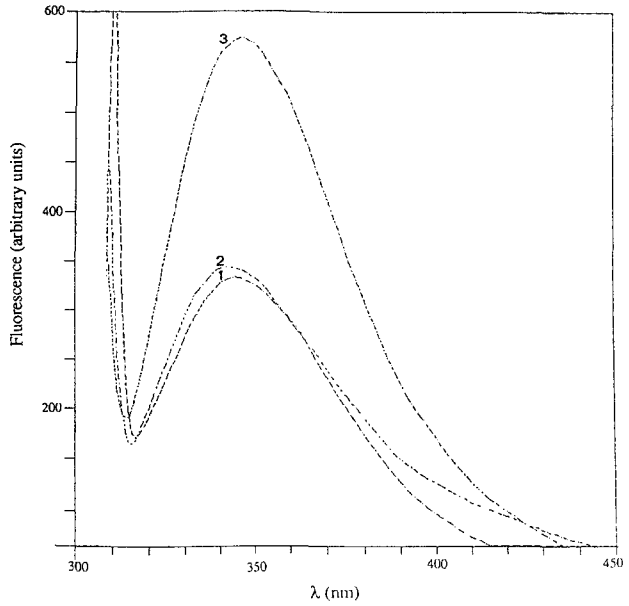

Fig. 2. Fluorescence emission spectra of the light chains. The spectra were recorded from 300 to 450 nm in 20 mM K phosphate buffer, pH 7.4 using a 0.44 μM protein concentration. Excitation was set at 295 nm. The spectra shown were obtained after correcting for the buffer spectrum. 1 = κ MOS; 2 = κ SCI; 3 = κ INC.

in PBS). After 1 h, kidneys were removed, diced, homogenized in PBS containing 15 mM PMSF, centrifuged at 10,000 rpm for 30 minutes at 4°C and reextracted 7 times until the A_{280} of the supernatant was < 0.10. The resultant pellet was homogenized in 1 ml of Laemmli sample buffer (40 mM Tris-HCl, 10 mM EDTA and 1% SDS, pH 8.0), boiled for 3 minutes and 10 μl of this solution were analyzed by SDS-PAGE electrophoresis according to Laemmli [11] using an acrylamide gradient 5–15%. The gel was blotted on immobilon membrane and immunostained with anti-κ antibodies as previously described [12] using the ECL system according to the manufacturer's suggestions.

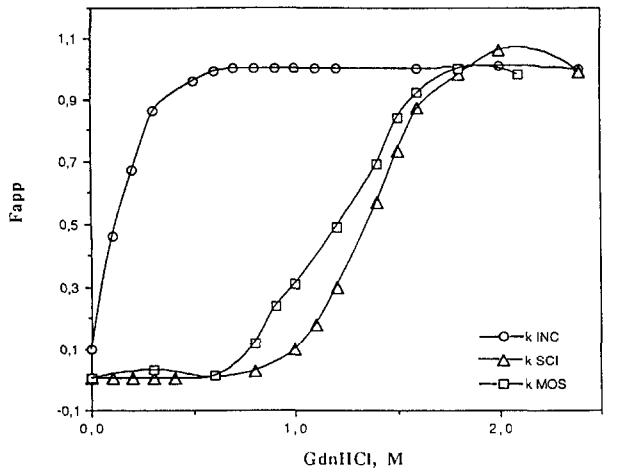

Fig. 3. Unfolding transition of the light chains induced by GdnHCl. Samples (0.44 μM in 10 mM K phosphate buffer and GdnHCl from 0 to 4 M, pH 7.4) were equilibrated at 20°C for 4 h before fluorescence was monitored. Excitation was set at 295 nm, emission at 345 nm. Data were the mean of three independent measurements and were converted to Fapp [15].

3. Results

3.1. Protein structure studies

The light chains used in the present study (MOS, SCI, INC) were obtained from human urine. Gel filtration analysis (Fig. 1) demonstrated that all the samples were dimers, free of high molecular weight contaminants accounting for light chain aggregates [18], as well as of light chain fragments frequently present in amyloidogenic Bence Jones proteins [15]. From the known primary structure, it appears

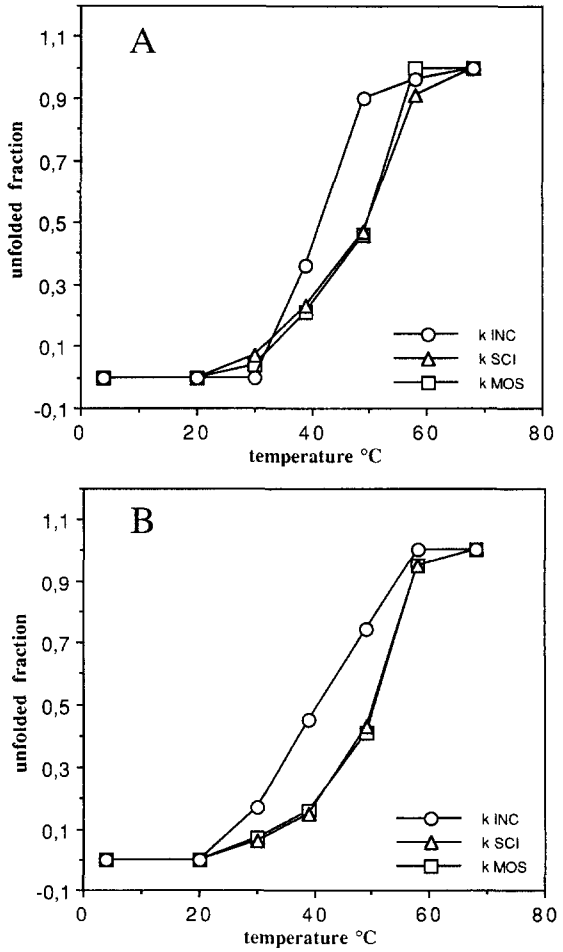

Fig. 4. Unfolding transition of the light chains induced by temperature. CD spectra were recorded at the indicated temperature in 20 mM K phosphate buffer, pH 4.0. Protein concentration was 2.2 μM in the far UV; 8.8 μM in the near UV. Unfolded fraction was calculated from the contribution of the ellipticity at 220 and 200 nm (A) and from the ellipticity at 280 nm (B). Fraction unfolded 1 = ellipticity at 70°C; 0 = ellipticity in the range 4–20°C. Data are the mean of three independent measurements.

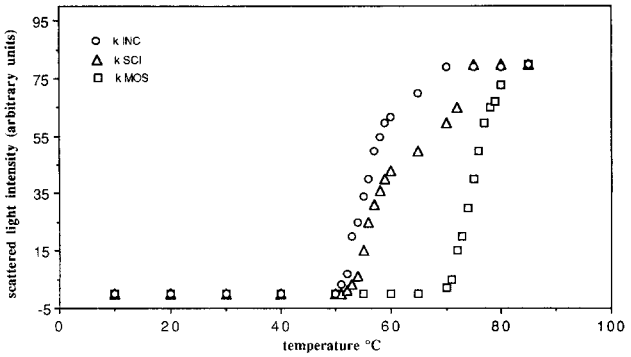

Fig. 5. Aggregation of the light chains induced by temperature. Light scattering was monitored at the indicated temperature in 20 mM K phosphate buffer, pH 4.0. Samples (13.2 μM) were excited at 510 nm and scattered light was detected at 90° to the incident beam.

that the amyloidogenic INC [10] is a κ II light chain constituted by 219 residues, and that κ SCI, associated with LCDD, is a 214-residue κ IIIa light chain [2]. Characterization of the non-pathogenic light chain MOS, accomplished by amino acid composition, molecular weight determination and N terminal sequence analysis (Table 1), indicates that this protein is also a complete κ I light chain. PAS stain of the three proteins, after PAGE electrophoresis, was negative thus excluding the presence of linked carbohydrates.

The isoelectrofocusing analysis gave the following values for the p*I* of the proteins: 6.4 (κ MOS); 6.9 (κ SCI); 4.4 (κ INC). Fluorescence analysis shows that the proteins have similar spectra, with a maximum centered between 340 and 350 nm (κ MOS = 344 nm, κ INC = 347 nm, κ SCI = 342 nm); however, the fluorescence intensity of κ INC in its native conformation is approximately double than that of SCI and MOS (Fig. 2), even though the Trp content is the same in these proteins.

In order to analyze the folding stability we characterized the response of the three light chains to GdnHCl by monitoring the unfolding-dependent increase in Trp fluorescence. Fig. 3 shows that κ SCI and κ MOS present

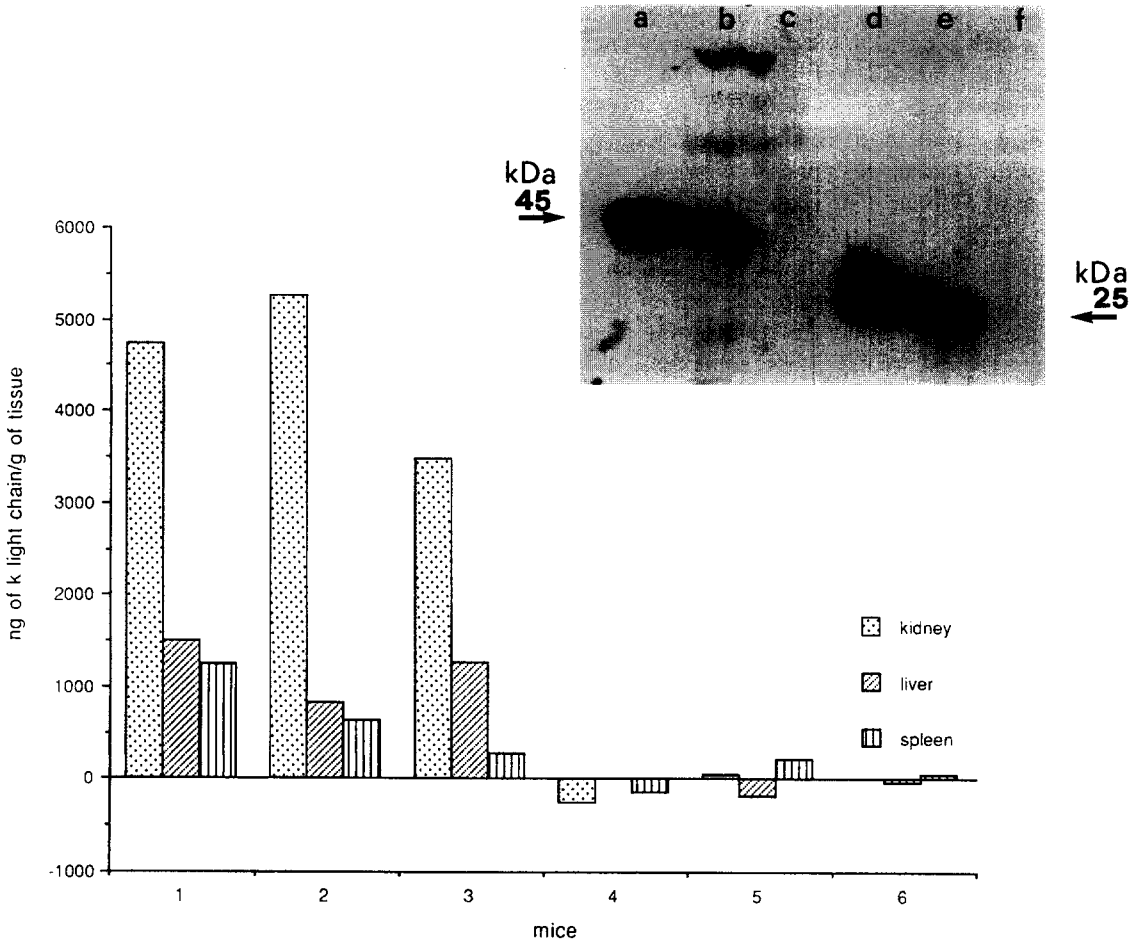

Fig. 6. Tissue deposition of the light chains. Mice 1, 2, 3 were injected with ^{125}I κ SCI and ^{131}I λ GAR; mice 4, 5, 6 were injected with ^{125}I κ MOS and ^{131}I λ GAR. Bound protein was quantified 1 h after the injection. See the Section 2 for detailed conditions. Inset: Immunoblotting was developed with anti human κ antiserum after a 5–15% SDS PAGE gradient. (a) 100 ng of purified κ SCI; (b) material extracted from the kidneys of a mouse injected with 0.5 mg of κ SCI in 0.5 ml of PBS; (c) material extracted from the kidneys of a mouse injected with 0.5 ml of PBS; (d-e-f) the same material as in lane a-b-c after reduction with 1 mM DTT.

very similar characteristics; their transition curves are sigmoidal and do not indicate a stable unfolding intermediate, suggesting that the proteins achieve the unfolded state through a single phase transition [19]. The calculated C_m was 1.35 M for κ SCI, 1.20 M for κ MOS. The $\Delta G_D^{H_2O}$, calculated as suggested by Pace et al. [19], was 5.6 kcal/mol for κ SCI and 5 kcal/mol for κ MOS.

In contrast, the amyloidogenic light chain INC appears to be an extremely unstable protein. Its unfolding midpoint is 0.1 M and the $\Delta G_D^{H_2O}$ was not calculated because an incomplete denaturation curve was obtained.

The effect of pH on the secondary structure of the three light chains was studied by measuring CD spectra in the far UV region, and the results were in good agreement with those obtained by Azuma et al. with κ and λ Bence Jones proteins [20]. The β sheet secondary structure is conserved in the three light chains in the range of pH 4–8, while a partially unfolded state is present at pH 3.0. At pH 2.0 the three immunoglobulins assume a random coil structure (data not shown).

The effect of the temperature at pH 4.0 was monitored in the near and far UV regions by raising the temperature from 20 to 70°C. The results illustrated in Fig. 4 show that in the far and in the near UV region the transition midpoint (T_m,) is 50°C for MOS and SCI and 40°C for INC. No aggregation can be observed, even in conditions of complete denaturation, at a protein concentration lower than 13.2 μM. Fig. 5 shows that at this concentration and pH 4.0, the aggregation of SCI and INC starts at very similar temperature (52°C and 50°C respectively), whereas a higher temperature is required for MOS (70°C). No fibrillar ultrastructure is visible by electron microscopy analysis of the insoluble precipitate. A small amount of fibrils were detected only in the case of κ INC after submitting its precipitate to pepsin digestion according to Linke et al. [16].

3.2. Tissue distribution of light chains in mice

The specific binding of κ SCI to mouse tissues is shown in Fig. 6. In all the treated animals, one hour after the intravenous injection of the labelled light chain, a significant amount of κ SCI is accumulated in the kidney, liver and spleen. The amount of protein in the kidney is 3 to 5 times higher than in the other two tissues.

Tissues were blindly analyzed by direct immunofluorescence with anti-κ and anti-λ light chains, which demonstrated faint κ chain deposition within the glomerulus and along the tubular and vascular basement membranes. Light microscopy findings were negative. No tissue deposition can be evidenced after injection of κ MOS, κ INC and λ GAR.

In separate experiments, the light chains SCI, INC and MOS were injected in mice and the material extracted from the kidneys was submitted to electrophoretic analysis. As shown in the insert of Fig. 6, after injection of κ SCI, a substantial amount of κ light chain is evidenced in the kidney extract. The data also indicate that the injected κ SCI is not significatively modified during kidney accumulation: it behaves as a dimer in non reducing conditions (lane b) and as a monomer after the addition of 1 mM DTT (lane e). Aspecific high molecular weight bands are also present in the control (see lane b and c). The material extracted from mice injected with light chain INC and MOS (data not shown) did not show any positive stain.

4. Discussion

The data obtained with our in vivo model evidence that the light chain SCI, responsible for LCDD, in its mature and dimeric form is deposited in kidney, liver and spleen. The kidney is more effective than the other tissues in retaining the radiolabelled protein. Moreover renal deposition of κ SCI appears to be a specific process: infact the control κ and λ light chains as well as the amyloidogenic κ INC are not retained even in this organ which is known to be the major metabolic site of these proteins [21]. Renal uptake of pathological light chains has also been observed by Solomon et al. [22] and Khamlichi et al. [23] using a different experimental protocol. Our data, in addition, point out the rapid accumulation of κ SCI in the kidney. As judged by the electrophoretic analysis, this process occurs without substantially remodelling of the protein structure. The absence of a lag phase in the kidney deposition of the LCDD associated protein might exclude a nucleation step which, on the contrary, seems to be necessary in amyloid formation [6].

Both the different deposition behaviour and the ultrastructural organization of the insoluble deposit focus attention on distinctive structural properties of the light chain responsible for the two diseases. Significant differences are evidenced in the present study by comparing some molecular properties of the light chains associated with AL amyloidosis and LCDD, with those of a non pathological counterpart.

The folding stability of κ SCI is similar to that of the non pathological κ MOS: C_m values of 1.35 and 1.20 M were obtained for the former and the latter respectively by monitoring the unfolding dependent increase of fluorescence as a function of denaturant concentration. These values agree with those previously reported by Rowe and Tanford [24] and Tsunenaga et al. [14] for non pathological light chains; both are slightly lower than that found for the recombinant VL domain of Rei light chain [7]. Similar stability is also evidenced by analysing the CD spectra of the proteins under different pH and temperature conditions. Both the proteins show considerable stability in the far UV range above pH 4.0. The effect of the temperature at this pH is identical: the two proteins go through a transition of the secondary and tertiary structure above 40°C. In contrast, as previously suggested on the basis of its primary

structure [10], κ INC is a very unstable protein; the C_m (0.1 M) is lower even with respect to that of the amyloidogenic point mutant R 61 of REI VL domain [7] in which the charged residue, as in INC [10], is replaced by an uncharged one. This behaviour and the high intrinsic fluorescence in non-denaturing condition suggest that Trp 95 is not completely quenched by the Cys 23-Cys 88 disulfide bridge [7], probably because a partially unfolded state is already present in the native protein. In accordance with the fluorescence data, the thermal denaturation of κ INC occurs about 10°C below with respect to the MOS counterpart. Thus amino acid replacements and folding instability appear to be related to the amyloid trait not only in transthyretin and cystatin mutants but also in a naturally occurring amyloid light chains. These data support the hypothesis that destabilizing amino acid replacements can induce a partially folded state prone to protein aggregation and fibril formation [7].

Although different in folding stability, the LCDD associated SCI and the amyloid INC share the property to self aggregate in vitro at 50°C under acidic conditions (pH 4.0). From the isoelectric point of the proteins it may be expected that the charge modification, induced by pH, may more affect INC than SCI self aggregation, since at this pH, the former may have a net charge near zero, the latter should be dissociated at a similar extent as the control. The review of the available primary structures of light chains responsible for LCDD has stand out the presence of unusual hydrophobic residues in positions generally occupied by hydrophilic or neutral amino acids [25]. This characteristic is shared by κ SCI which presents Ile in position 53 and 77 respectively occupied by Asn and Ser in REI light chain and generally by polar residues in κ and λ light chains. This suggests that the presence of such a bulky apolar side chains that, according to the X ray structure of κ REI [26], are both located in regions exposed to the solvent, may prime the aggregation of the unfolded protein through intermolecular hydrophobic interactions.

In conclusion, the rapid and specific tissue accumulation and the tendency to in vitro aggregation of the protein in its unfolded state, support the hypothesis that deposition of the LCDD associated κ SCI may occur in vivo through a two step process. At the beginning the monoclonal light chain binds a still unknown component of the basement membrane, accumulates and reach a high concentration in the kidney; later on, protein aging and local conditions could cause unfolding and self aggregation that enhance the deposition of insoluble light chain precipitate.

Acknowledgements

We would like to thank Dr. G. Mellerio for allowing us to use the spectrofluorimeter and spectropolarimeter at the 'Centro Grandi Strumenti of the University of Pavia', and Dr.ssa A. Cobianchi for her skillful technical assistance. This work was supported by grants from Ministero dell' Università della Ricerca Scientifica e Tecnologica and from CNR, Rome, Italy.

References

[1] Gallo, G., Picken, M., Buxbaum, J. and Frangione, B. (1989) Sem. Hematol. 26, 234–235.
[2] Bellotti,V., Stoppini, M., Merlini, G., Zapponi, M.C., Meloni, M., L., Banfi, G. and Ferri, G. (1991) Biochim. Biophys. Acta. 1097, 177–182.
[3] Cognè, M., Preud'homme, J.L., Bauwens, M., Touchard, G. and Aucouturier, P. (1991) J. Clin. Invest. 87, 2186–2190.
[4] Khamlichi, A.A., Aucouturier, P., Silvain, C., Bauwens, M., Touchard, G., Preud'homme, J.L., Nau, F. and Cognè, M. (1992) Clin. Exp. Immunol. 87, 122–126.
[5] Rocca, A., Khamlichi, A.A., Aucouturier, P., Noel, L.H., Denoroy, L., Preud'homme, J.L. and Cognè, M. (1993) Clin. Exp. Immunol. 91, 506–509.
[6] Stevens, F.J., Myatt, E.A., Chang, C.H., Westholm, F.A., Eulitz, M., Weiss, D.T., Murphy, C., Solomon, A. and Schiffer, M. (1995) Biochemistry 34, 10697–10702.
[7] Hurle, M.R., Helms, L.R., Li, L. and Wetzel, R. (1994) Proc. Natl. Acad. Sci. USA 91, 5446–5450.
[8] McCutchen, S., Zhihong, L., Miroy G.J., Kelly, J.W. and Colon, W. (1995) Biochemistry 34, 13527–13536.
[9] Abrahamson, M. and Grubb, A. (1994) Proc. Natl. Acad. Sci. USA 91, 1416–1420.
[10] Ferri, G., Stoppini, M., Iadarola, P., Bellotti, V. and Merlini, G. (1989) Biochim. Biophys. Acta 995, 103–108.
[11] Laemmli, U.K. (1970) Nature 227, 680–685.
[12] Bellotti, V., Merlini, G., Bucciarelli, E., Perfetti, V., Quaglini, S. and Ascari, E. (1990) Brit. J. Haematol. 74, 65–69.
[13] Moore, S. (1968) J. Biol. Chem. 243, 6281–6283.
[14] Tsunenaga, M., Goto, Y., Kawata, Y. and Hamaguchi, K. (1987) Biochemistry 26, 6044–6051.
[15] Finn, B. E., Chen, X., Jennings, P.A., Saalau-Bethell, S.M. and Matthews, C.R. (1992) in: Protein Engineering (Rees, A.R., Stenderberg, M.J.E. and Wetzel, R., eds.), pp. 167–189, IRL, Oxford Univ. Press, Oxford.
[16] Linke, R.P., Zucker-Franklin, D. and Franklin, E.C. (1973) J. Immunol. 111, 10–23.
[17] Wilson, C.B. and Dixon, F.J. (1971) J. Exp. Med. 134, 7–18.
[18] Myatt, E.A., Westholm, F.A., Weiss, D.T., Solomon, A., Sciffer, M. and Stevens, F. (1994) Proc. Natl. Acad. Sci. USA 91, 3034–3038.
[19] Pace, C.N. (1986) Methods Enzymol. 131, 266–280
[20] Azuma, T., Hamaguchi, K. and Migita, S. (1972) J. Biochem. 71, 379–386.
[21] Wochner, R.D., Strober, W. and Waldmann, T.A. (1967) J. Exp. Med. 126, 207–221.
[22] Solomon, A., Weiss, D.T. and Kattine, A.A. (1991) N. Engl. J. Med. 324, 1845–1851.
[23] Khamlichi, A.A., Rocca, A., Touchard, G., Aucouturier, P., Preud'homme, J.L. and Cognè, M. (1995) Blood 86, 3655–3659.
[24] Rowe, E.S. and Tanford, C. (1973) Biochemistry 24, 4822–4827.
[25] Preud'homme, J.L., Aucouturier, P., Touchard, G., Striker, L., Khamlichi, A.A., Rocca, A., Denoroy, L. and Cognè, M. (1994) Kidney Int. 46, 965–972.
[26] Epp, O., Lattman, E.E., Schiffer, M., Huber, R. and Palm, W. (1975) Biochemistry 14, 4943–4952.